Study of *pp* interactions at high multiplicity at U-70

A. Aleev, V. Avdeichikov, V. Balandin, Yu. Borzunov, Yu. Chencov, V. Dunin, N. Furmanec, G. Kekelidze, V. Kireev, E. Kokoulina, V. Ladygin, V. Myalkovsky, V. Nikitin, V. Peshehonov, Yu. Petukhov, I. Rufanov, A. Yukaev, N. Zhidkov

JINR, VBLHE, Dubna, Moscow region, Russia, 141980

S. Basiladze, G. Bogdanova, I. Erofeeva, N. Grishin, Ya. Grishkevich, D. Karmanov, V. Kramarenko, A. Leflat, M. Merkin, V. Popov, L. Tihonova, A. Vishnevskaya, V. Volkov,A. Voronin, E. Zverev

Lomonosov Moscow State University Scobeltsyn Institute of Nuclear Physics, Russia, 110000

E. Ardashev, A. Afonin, V. Golovkin, S. Golovnya, S. Gorokhov, A. Kholodenko, A. Kiryakov, L. Kurchaniniv, I.Lobanov, E. Lobanova, G. Mitrofanov, V.Petrov, A. Pleskach, M. Polkovnikov, V. Ronzhin, V. Ryadovikov, V. Senko, M. Soldatov, N. Shalanda,Yu. Tsyupa, A. Vorobiev, V. Yakimchuk, V. Zapolsky,

IHEP, Protvino, Russia, 142281

A. Kutov

DM Komi SC UrD RAS, Syktyvkar, Russia 167982

The E190 Experiment is aimed at the search for collective phenomena in a quark-gluon system and a hadron system. It is carried out at U-70 in IHEP, Protvino. The evidence of Bose-Einstein condensation of pions has been confirmed with a twofold increasing of sampling at a level of 7 standard deviations. We study soft photon (smaller than 60 MeV) yield by using of an electromagnetic calorimeter with low energy threshold. In the gluon dominance model we explain multiparticle production by the active gluons. In this model the estimation of the contribution of charge exchange has been obtained.

1. Introduction

Our SVD-2 Collaboration carries out the experiment E-190 at the U-70 accelerator of IHEP [1] in Protvino city near Moscow. There are three main participants: Lomonosov MSU SINP, IHEP, and JINR. Our project is aimed at studying of *pp* interactions with 50 GeV/c proton beam. We are interested in investigation of high multiplicity (HM) events. HM is considerably higher than average multiplicity. We tend to reach the kinematical limit. The kinematical limit is defined by a condition of the transformation of the whole kinetic energy into mass of secondary pions. Pions are copiously formed at the U-70 energies 50–70 GeV.

Almost all Monte Carlo event generators are mistaken when they make predictions for HM region. PYTHIA underestimates two orders of magnetude topological cross section at $N_{ch} = 18$ (the Mirabelle Collaboration data) [1]. Models give diverse predictions too [1]. We believe that the HM study will give the deeper understanding of multi particle production mechanism.

Section 2 is devoted to HM phenomenology. The description of this region is carried out in the framework of the gluon dominance model (GDM) [3]. This model improves description of topological cross sections in this region, estimates the charge exchange contribution. The evidence of pion condensate formation is presented in section 3. The preparation for soft photon yield study is presented in section 4. Section 5 states the conclusions.

2. Phenomenology of high multiplicity

We carry out studies at the Spectrometer with Vertex Detector (SVD) setup [1] which consists of a hydrogen target, a high multiplicity trigger, a vertex detector, a drift tube chamber, a magnetic spectrometer (magnet and proportional chambers) and an electromagnetic calorimeter (ECal). We can register both charged and neutral particles. To measure of soft photons we included in the SVD setup a soft photon electromagnetic calorimeter (SPEC).

To suppress the registration of low multiplicity events the scintillator hodoscope or HM trigger has been manufactured. At trigger level $l =$ 4, 6, 8, 10, 12 we register events with multiplicity no less than the given level [2]. One million events have been processed at $l = 8$ with taking into account corrections obtained by a Monte-Carlo simulation. Topological cross sections and average multiplicity have been obtained [1].

To describe previous data and make predictions in the HM region we have developed a gluon dominance model (GDM) [3–6]. This model has appeared from the two stage model describing multiplicity distributions in e^+e^- annihilation at high energies by two stages [7]. The first stage is based

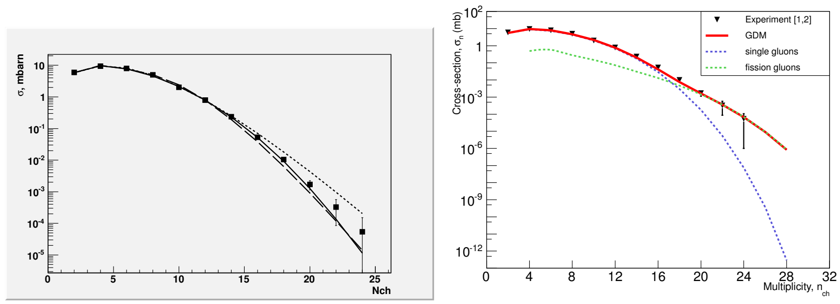

Fig. 1. Left panel: Experimental topological cross sections and the predictions of IHEP model [9], NBD and GDM. Right panel: Topological cross section versus charged multiplicity in GDM [3]. The dashed blue line describes the contribution of single sources, the green line – sources consisted of two gluons of fission, the solid red line is the sum both of contributions.

on QCD quark-gluon cascade: gluon bremsstrahlung by quarks and gluon fission. This stage is described by negative binomial distribution (NBD). The second stage (hadronization) is based on the phenomenological scheme with use of a binomial distribution.

Convolution of the two stages gives good agreement with the data in the region from 10 up to 200 GeV. The main result of that description is constancy of hadronization parameter $\overline{n}_g^h$. It defines the average number of charged particles nascent from one gluon source through itself passing of the hadronization stage. Such behavior is the evidence of the fragmentation mechanism of hadronization in e^+e^- annihilation: one parton — one hadron [8].

It has been shown in the framework of GDM that initial quarks are staying in leading particles and multi particle production is realized by active gluons. Two scheme were proposed with and without inclusion of a gluon fission. Gluon branching is described by a Farry distribution. In both schemes parameters of hadronization grow and become more than 1. We observe their growth from 1.5 at 50 GeV/c, U-70, up to 3.3 at 62 GeV, ISR. In the scheme with fission some gluons do not turn into hadrons (about 50 %) and stay in a quark-gluon system. They can be the sources of anomalous soft photons. GDM describes and predicts topological cross sections of pp ($p\overline{p}$) interactions in HM region. Topological cross sections and their model descriptions are shown in the left panel of Fig.1. The model of IHEP [9] (a dashed line) and GDM (a solid line) describe data well, NBD (a dotted line) overestimates of them slightly in HM area.

In double-logarithmic approximation the emission of two gluons can explain the angle broadening [10]. One of them is a product of fission. At U-70 this fission can occur. In the right panel of Fig. 2 contributions of two types of sources is shown. The blue dashed line describes contribution of single gluon sources, the green dashed line — double gluon sources nascent as a result of fission of single gluons and the red solid line is the superposition both contributions. The accounting of gluon fission improves the description of HM tail.

In the framework of GDM one can estimate the charge exchange contribution at $n_{ch} = 2$. One of the two protons can pass its charge to a neutral meson with turning it into a charged meson

$$p + p \to p + \pi^+ + n + N_\pi. \tag{1}$$

The cross section $\sigma_{2\to 2}$ consists of elastic and inelastic cross sections: $\sigma_{2\to 2} = \sigma_{2,el} + \sigma_{2,inel}$, where $\sigma_{2,inel}$ in turn consists of two summands, one of them is responsible for the charge exchange ($\sigma_2^{(+ch)}$), the second one ($\sigma_2^{(-ch)}$) for the inelastic cross section without it. GDM does not take into account the charge exchange. So we express $\sigma_{2,inel}$ through parameter P: $\sigma_{2,inel} = P \cdot \sigma_2^{(-ch)}$, as we know how $\sigma_2^{(-ch)}$ is calculated in GDM. Then we describe data by GDM in the whole multiplicity region, find GDM's parameters and P. Hence we estimate the charge exchange coefficient as $q = \sigma_2^{(+ch)}/\sigma_{2,inel} \cdot 100\%$ It approximates 50$\pm$ 5%. This value is comparable with the data [11].

3. Search for collective phenomena at U-70

V. Begun and M. Gorenstein have predicted the conditions of the Bose-Einstein Condensate (BEC) formation for pp interactions at U-70 at high total multiplicity, $N_{tot} = N_{ch} + N_0$, in the framework of the ideal pion gas model [12]. N_0 is a number of neutral pions. The growth of total multiplicity leads to decrease of the pion system temperature. Pions are bosons and can fall out in pion condensate at high multiplicity.

The indication at the BEC formation is a growth of neutral pion number fluctuations. Begun and Gorenstein have proposed to measure the scaled variance. The scaled variance is calculated by the definition

$$\omega = D/ < N_0 >,$$

where $D =< (N_0- < N_0 >)^2 >$ is a variance of neutral meson number, $N_{tot} = N_{ch} + N_0$ is fixed. $\omega = 1$ in the case of Poisson distribution. They have predicted [12] that the fluctuations of π^0 and $\pi^\pm$ number increases dramatically and abruptly when the system approaches the BEC line at the thermodynamic limit and $\omega \to \infty$. In the system of limited size a scaled variance grows to the certain constant value. The BEC temperature for

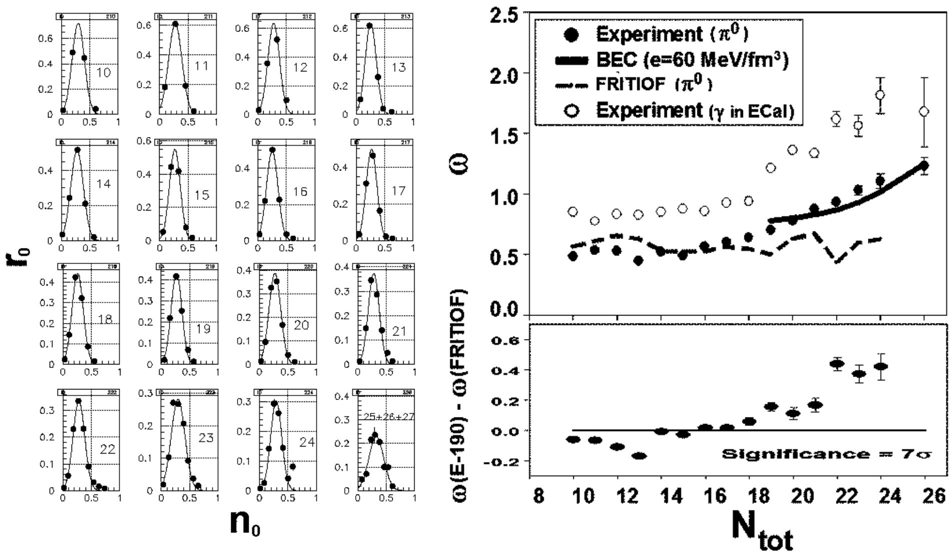

Fig. 2. Left panel. Multiplicity distributions of π^0-mesons versus the scaled total multiplicity at different total multiplicity. Right panel. (Top) The measured scaled variance ω versus N_{tot} for π^0-mesons ($\bullet$), photons ($\circ$), MC code FRITIOF7.02 (the dashed curve) and theoretical prediction (solid curve) [12] for the energy density ε =60 MeV/fm^3. $N_{tot} = N_{ch} + N_0$ for π^0-mesons and $N_{tot} = N_{ch} + N_\gamma$ for photons. (Bottom) The difference of experimental and Monte Carlo simulated ω for π^0-mesons [14, 15].

a pion system is considerably more than for a nuclear system as radius of nuclei is considerably bigger pion size [13].

Owing to the improved method of the photon registration the multiplicity distributions of π^0-mesons have been restored. To compare their at different values of total number of pions the scaled multiplicity n_0 is used. It is determined by the ratio $n_0 = N_0/N_{tot}$ and variates in the region $0 \le n_0 \le 1$. The distributions of neutral pions, $r_0(n_0, N_{tot})$ are presented in the left panel of Fig. 2. The experimental values of the scaled variance have shown the growth about seven standard deviations to a comparison with Monte-Carlo generators. It is seen in the right panel of Fig. 2. The same growth we observe for scaled variance versus a variable $N_{tot} = N_{ch} + N_\gamma$.

An interesting explanation of the connection between BEC and excess of soft photon yield has been proposed by S. Barshay [16].

4. Study of Soft Photon yield

Photons interact with nuclear matter only electromagnetically, and therefore they bear the information on properties of the environment during the interaction. The direct photons are not decay products of any known particles. In accordance with quantum electrodynamics they may be emitted in the process of charged particle scattering – bremsstrahlung at a hadron or parton cascade. In particular, $q + g \rightarrow q + \gamma$ parton interactions lead to photon emission. The higher the density and the longer the system lifetime, the more direct photons should be emitted. These photons are useful probes to investigate nuclear matter at all stages of the interaction.

Special attention is devoted to low energy direct soft photons (SP) which yield surpasses the theoretical predictions [17–19]. This excess is observed in K^+p, $\pi^{\pm}p$, $p\overline{p}$ and pA interactions from 10 GeV up to 450 GeV. Experimental and theoretical studies of the direct photon production in hadronic collisions essentially expand our insights into multi particle production [20]. SP have low transverse and longitudinal momenta $p_T < 0.1$ GeV/c and $|x| < 0.01$. In this domain their yield exceeds the theoretical estimates by 5–8 [17, 18] times and even 17 for neutral pions [19]. The phenomenological models try to explain this excess. Until now, no model was able to explain the experimental data well as a whole, especially in a kinematic range where the effect is most prominent [21].

SVD Collaboration has manufactured SPEC with low energy threshold. The main feature is its capability to register low energy deposit $E \leq 1$ MeV. Up to now none of the known experiments has reached such low value of the photon energy detection. It is presented in the left panel of Fig. 3. The calorimeter is the matrix of 49 scintillator counters. Every counter consists of BGO crystal. The crystal size is equal to $30{\times}30{\times}180$ mm^3. Photomultipliers (PMT) of type 9106SB (ET Enterprizes) look over the end face of every scintillator. PMT have 7 dynodes and green extended quantum efficiency. The diameter of photocathode is 25 mm, the diameter of the bulb is not more than 29.5 mm. The bulb has integrated permalloy shield. The PMT is fixing on the crystal by optic glue EPO-TEK 301.

The preliminary amplifier is manufactured on the current feedback (CFB) operational amplifier (OA) Ad8014. The signals from PMT is given to the inverting entry of OA. The maximum value of signal to noise ratio (SNR) is reached by minimal input capacitance on the OA input. This capacitance is defined by dynode-anode gap and assembling capacitance and is about 6 pF. The dynamic range of signals is more than 66 dB.

The front and back sides of the intermediate transitional plates are connected between themselves by two stubs of cables. One of them is placed into the box with crystals, another — out of the box. The low voltage bias

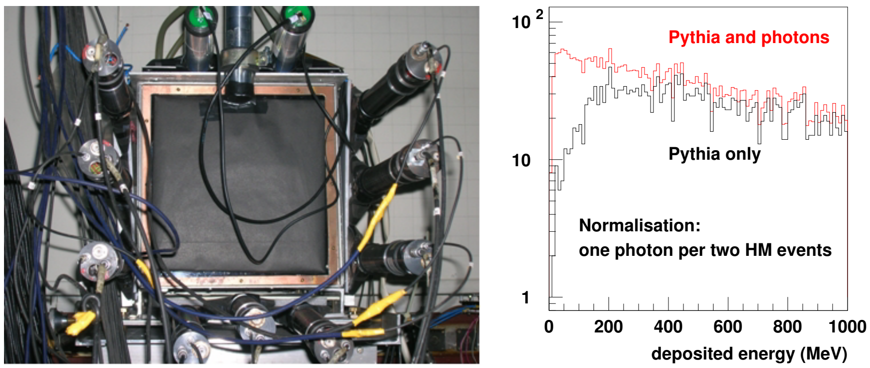

Fig. 3. Left panel: Soft photon electromagnetic calorimeter (SPEC). Right panel: Monte-Carlo energy spectra of photons in pp interactions.

(+6 V and -6 V) for the preamplifiers and HV (400-600 V) for PMT are generating on the distributive mother board .

High voltage can regulate on the external plate for every column of assembly (seven elements). The internal plate connects with back wall of calorimeter shield with using of three stubs. The commutations of counters with signal cable lines leading to electronics is carried out by these stubs and located at the control panel of setup.

The feeding of SPEC is realized by two sources +12 V and - 12 V. At the current of consumption smaller than 1 A (+12 V) and 50 mA (-12 V). PMT have been included in scheme with grounded photocathode. Such inclusion is explained by the maximum density of the packing of crystals. The signals is acquired from amplifiers arrive to amplifier inputs through cable lanes which are located on the control desk next to the data acquisition system electronics. After inversion every signal is divided into two and is digitized. One channel is direct, second – observable. The attenuation coefficient is 1:1.5. There are 112 output channels. The calorimeter is placed into the thermo-statical box. The thermal stabilization is realized by Huber 006B setup. The temperature is chosen 18 °C. The calorimeter is surrounded with scintillator counters of a guard system and a passive neutron protection by 8 cm-thickness polyethylene.

The Monte-Carlo simulation of assembly with all crystals is shown in the left panel of Fig. 3. The black line presents the simulation by PYTHIA without SP contribution, the red line takes into account SP contribution by Low formula, $d\sigma/dp \sim 1/p$.

We had a test run this year. The new calorimeter has been put near ECal under 2–6 ° and at the distance of 11 m from a hydrogen target. In the right panel of Fig. 3 the signal spectra in the calorimeter is presented. It has been obtained at the next conditions: there is no signal in the veto system; there are no signals in counters of the external layer. The signals in the internal part of assembly (3×3 crystals) were summed up on all 9 channels with weight coefficients definite at the calibration. The soft photon spectra has been obtained. Its analysis is in progress. Now we plan to transfer SP study at Nuclotron, JINR.

Acknowledgments

We appreciate all participants of the SVD-2 Collaboration for their active and fruitful work.

References

[1] V.N. Ryadovikov, Phys. Atom. Nucl. **75**, 315 (2012).

[2] E. Kokoulina, A. Kutov, V. Nikitin, Y. Petukhov, and V. Popov, Proceedings of the 40th ISMD, Antwerpen University, 115 (2011).

[3] E.S. Kokoulina, Acta Phys. Pol. B **35**, 295 (2004).

[4] E.S. Kokoulina and A.A. Nikitin, Proc. of the 17th ISHEPP: Dubna, Russia, 319 (2006).

[5] P.F. Ermolov *et al.*, Proc. of the 17th ISHEPP, Dubna, Russia, 327 (2006).

[6] E.S. Kokoulina, AIP Conference proceeding, **828**, 81 (2006).

[7] E.S. Kokoulina, XXXII ISMD, Alushta, Ukraine, W. Sc. 340 (2002).

[8] B. Muller, Nucl. Phys. A **750**, 84 (2005).

[9] S.V. Semenov *et al.*, Sov. J. Nucl. Phys. **22**, 410 (1975).

[10] E.A. Kuraev, S. Bakmaev, and E.S. Kokoulina, Nucl. Phys. B **851**, 551 (2011).

[11] S. Bascovich *et al.*, Yad. Phys. (Russian) **27**, 1225 (1978).

[12] V.V. Begun and M.I. Gorenstein, Phys. Lett. B **653**, 190 (2007).

[13] V.V. Begun and M.I. Gorenstein, Phys.Rev. C **78**, 024904 (2008).

[14] E.S. Kokoulina, Prog. Theor. Phys. Suppl. **193**, 306 (2011).

[15] A.G. Afonin *et al.*, Eur. Phys. J. Web Conf. **37**, 06002 (2012); E. Kokoulina, PoS ICHEP2012, 259 (2013); E.S. Kokoulina *et al.*, PoS Baldin-ISHEPP-XXI, 007 (2012).

[16] S. Barshay, Phys. Lett. B **227**, 279 (1989).

[17] P.V. Chliapnikov *et al.*, Phys. Lett. B **141**, 276 (1984).

[18] A. Belogianni *et al.*, Phys. Lett. B **548**, 129 (2002).

[19] J. Abdallah *et al.*, Eur. Phys. J. C **67**, 343 (2010).

[20] http://theor.jinr.ru/twiki-cgi/view/NICA/NICAWhitePaper.

[21] P. Lichard, Phys. Rev. D **50**, 6824 (1994).